

Provably Correct Training of Neural Network Controllers Using Reachability Analysis

Xiaowu Sun¹ Yasser Shoukry¹

Abstract—In this paper, we consider the problem of training neural network (NN) controllers for cyber-physical systems (CPS) that are guaranteed to satisfy safety and liveness properties. Our approach is to combine model-based design methodologies for dynamical systems with data-driven approaches to achieve this target. Given a mathematical model of the dynamical system, we compute a finite-state abstract model that captures the closed-loop behavior under all possible neural network controllers. Using this finite-state abstract model, our framework identifies the subset of NN weights that are guaranteed to satisfy the safety requirements. During training, we augment the learning algorithm with a NN weight projection operator that enforces the resulting NN to be provably safe. To account for the liveness properties, the proposed framework uses the finite-state abstract model to identify candidate NN weights that may satisfy the liveness properties. Using such candidate NN weights, the proposed framework biases the NN training to achieve the liveness specification. Achieving the guarantees above, can not be ensured without correctness guarantees on the NN architecture, which controls the NN’s expressiveness. Therefore, and as a corner step in the proposed framework is the ability to select provably correct NN architectures automatically.

I. INTRODUCTION

The last decade has witnessed tremendous success in using machine learning (ML) in a multitude of safety-critical cyber-physical systems domains, such as autonomous vehicles, drones, and smart cities. Indeed, end-to-end learning is attractive for the realization of feedback controllers for such complex cyber-physical systems, thanks to the appeal of designing control systems based on purely data-driven architectures. However, regardless of the explosion in the use of machine learning to design data-driven feedback controllers, providing formal safety and reliability guarantees of these ML-based controllers is in question. It is then unsurprising the recent focus in the literature on the problem of safe and trustworthy autonomy in general, and safe reinforcement learning, in particular.

The literature on the safe design of ML-based controllers for dynamical and hybrid systems can be classified according to three broad approaches, namely (i) incorporating safety in the training of ML-based controllers, (ii) post-training verification of ML-based controllers, and (iii) online validation of safety and control intervention. Representative examples of the first approach include reward-shaping [1], Bayesian and robust regression [2], [3], [4], and policy optimization with constraints [5], [6], [7], [8]. Unfortunately, this approach does

not provide provable guarantees on the safety of the trained controller. Other techniques in this domain include Lyapunov methods [9], [10], [11], and safe model predictive control [12] which focuses mainly on providing stability guarantees rather than general safety and liveness guarantees.

To provide strong safety and reliability guarantees, several works in the literature focus on applying formal verification techniques (e.g., model checking) to verify pre-trained ML-based controllers’ formal safety properties. Representative examples of this approach are the use of SMT-like solvers [13], [14], [15] and hybrid-system verification [16], [17], [18]. However, these techniques only assess a given ML-based controller’s safety rather than design or train a safe agent.

Due to the lack of safety guarantees on the resulting ML-based controllers, researchers proposed several techniques to *restrict* the output of the ML-based controller to a set of safe control actions. Such a set of safe actions can be obtained through reachability analysis [19], [20], [21], barrier certificates [22], [23], [24], [25], [26], [27], [28], [29], [30], and online learning of uncertainties [31]. Unfortunately, methods of this type suffer from being computationally expensive, specific to certain controller structures or else employ training algorithms that require assumptions on the system model.

This paper proposes a principled framework combining model-based control and data-driven neural network training to achieve enhanced reliability and verifiability. Our framework bridges ideas from reachability analysis to guide and bias the neural network controller’s design and training and is capable of supplying strong reliability guarantees. To that end, and starting from a nonlinear model of the system, we compute a finite-state abstract model capable of capturing the closed-loop behavior under *all* neural network controllers. Such a finite-state abstract model can be computed using a direct extension of existing reachability tools. Next, our framework uses this abstract model to search for *safe* subsets of neural network weight assignments that are guaranteed to result in a safe controller. During the neural network training, we use a novel *projection* operator that projects the trained neural network weights to the subsets found to be safe.

Unlike the safety property, satisfying the liveness property can not be enforced by projecting the trained neural network weights. Therefore, to account for the liveness properties, our framework utilizes the abstract model further to refine the safe set of neural network weights to find sets of *candidate* NN weights that may satisfy the liveness properties. The framework then ranks these *candidates* and bias the NN training process accordingly until a NN that satisfies the liveness property is obtained. In conclusion, the contributions

¹Department of Electrical Engineering and Computer Science, University of California, Irvine, CA 92697 USA {xiaowus, yshoukry}@uci.edu

This work was partially sponsored by the NSF awards #CNS-2002405 and #CNS-2013824.

of this paper can be summarized as follows:

- 1) An abstraction-based framework that captures the behavior of *all* possible neural network controllers.
- 2) A novel NN weight projection operator that can be integrated with any NN training procedure to ensure that the trained NN is provably safe.
- 3) A procedure to bias the NN training to satisfy the liveness properties.

II. PROBLEM FORMULATION

Notation: The symbols \mathbb{R} and \mathbb{N} denote the set of real and natural numbers, respectively. The symbols \wedge and \implies denote the logical AND and logical IMPLIES, respectively. We use $\Psi_{\text{CPWA}} : \mathcal{X} \rightarrow \mathbb{R}^m$ to denote a Continuous and Piece-Wise Affine (CPWA) function of the form:

$$\Psi_{\text{CPWA}}(x) = K_i x + b_i \quad \text{if } x \in \mathcal{R}_i, \quad i = 1, \dots, L, \quad (1)$$

where the polytopic sets $\{\mathcal{R}_1, \dots, \mathcal{R}_L\}$ is a partition of the set \mathcal{X} . We call each polytopic set $\mathcal{R}_i \subset \mathcal{X}$ a linear region, and use $\mathbb{L}_{\Psi_{\text{CPWA}}} = \{\mathcal{R}_1, \dots, \mathcal{R}_L\}$ to denote the set of linear regions associated to Ψ_{CPWA} .

A. Dynamical Model, Neural Network Controller, and Specification

Consider discrete-time nonlinear dynamical systems of the form:

$$x^{(t+1)} = f(x^{(t)}, u^{(t)}), \quad (2)$$

where the state vector $x^{(t)} \in \mathcal{X} \subset \mathbb{R}^n$, the control vector $u^{(t)} \in \mathcal{U}$, and $t \in \mathbb{N}$. Given a feedback control law $\Psi : \mathcal{X} \rightarrow \mathcal{U}$, we use $\xi_{x_0, \Psi} : \mathbb{N} \rightarrow \mathcal{X}$ to denote the closed-loop trajectory of (2) that starts from the state $x_0 \in \mathcal{X}$ and evolves under the control law Ψ .

In this paper, our primary focus is on controlling the nonlinear system (2) with a state-feedback neural network controller $\mathcal{NN} : \mathcal{X} \rightarrow \mathcal{U}$. A K -layer Rectified Linear Unit (ReLU) NN is specified by composing K layer functions (or just layers). A layer l with i_l inputs and o_l outputs is specified by a weight matrix $W^{(l)} \in \mathbb{R}^{o_l \times i_l}$ and a bias vector $b^{(l)} \in \mathbb{R}^{o_l}$ as follows:

$$L_{\theta^{(l)}} : z \mapsto \max\{W^{(l)}z + b^{(l)}, 0\}, \quad (3)$$

where the max function is taken element-wise, and $\theta^{(l)} \triangleq (W^{(l)}, b^{(l)})$ for brevity. Thus, a K -layer ReLU NN is specified by K layer functions $\{L_{\theta^{(l)}} : l = 1, \dots, K\}$ whose input and output dimensions are composable: that is they satisfy $i_l = o_{l-1} : l = 2, \dots, K$. Specifically:

$$\mathcal{NN}_{\theta}(x) = (L_{\theta^{(K)}} \circ L_{\theta^{(K-1)}} \circ \dots \circ L_{\theta^{(1)}})(x), \quad (4)$$

where we index a ReLU NN function by a list of matrices $\theta \triangleq (\theta^{(1)}, \dots, \theta^{(K)})$. Also, it is common to allow the final layer function to omit the max function altogether, and we will be explicit about this when it is the case.

Specifying the number of layers and the dimensions of the associated matrices $\theta^{(l)} = (W^{(l)}, b^{(l)})$ specifies the architecture of the ReLU NN. Therefore, we use:

$$\mathcal{A} \triangleq ((n, o_1), (i_2, o_2), \dots, (i_{K-1}, o_{K-1}), (i_K, m)) \quad (5)$$

to denote the architecture of a ReLU NN. Given a NN architecture \mathcal{A} , we denote by $\Theta_{\mathcal{A}}$ the set of all lists of matrices θ that satisfy the number of layers and dimensions required by \mathcal{A} :

$$\Theta_{\mathcal{A}} \triangleq \{\theta = (\theta^{(1)}, \dots, \theta^{(K)}) \mid \theta^{(l)} = (W^{(l)}, b^{(l)}), W^{(l)} \in \mathbb{R}^{o_l \times i_l}, b_l \in \mathbb{R}^{o_l}\}. \quad (6)$$

As a typical control task, this paper considers a reach-avoid specification ϕ , which combines a safety property ϕ_{safety} for avoiding a set of obstacles $\{\mathcal{O}_1, \dots, \mathcal{O}_o\}$ with $\mathcal{O}_i \subset \mathcal{X}$, and a liveness property ϕ_{liveness} for reaching a goal region $\mathcal{X}_{\text{goal}} \subset \mathcal{X}$ in a bounded time horizon T . We use $\xi_{x_0, \Psi} \models \phi_{\text{safety}}$ and $\xi_{x_0, \Psi} \models \phi_{\text{liveness}}$ to denote a trajectory $\xi_{x_0, \Psi}$ satisfies the safety and liveness specifications, respectively, i.e.:

$$\begin{aligned} \xi_{x_0, \Psi} \models \phi_{\text{safety}} &\iff \forall t \in \mathbb{N}, \forall i \in \{\mathcal{O}_1, \dots, \mathcal{O}_o\}, \xi_{x_0, \Psi}(t) \notin \mathcal{O}_i, \\ \xi_{x_0, \Psi} \models \phi_{\text{liveness}} &\iff \exists t' \in \{1, \dots, T\}, \xi_{x_0, \Psi}(t') \in \mathcal{X}_{\text{goal}}. \end{aligned}$$

Given a set of initial states $\mathcal{X}_{\text{init}}$, a control law $\Psi : \mathcal{X} \rightarrow \mathbb{R}^m$ satisfies the specification ϕ (denoted by $\Psi, \mathcal{X}_{\text{init}} \models \phi$) if all trajectories starting from the set $\mathcal{X}_{\text{init}}$ satisfy the specification, i.e., $\xi_{x, \Psi} \models \phi, \forall x \in \mathcal{X}_{\text{init}}$.

B. Main Problem

Given the dynamical model (2) and a reach-avoid specification $\phi = \phi_{\text{safety}} \wedge \phi_{\text{liveness}}$, we consider the problem of designing an NN controller with provable guarantees as described in the next problem.

Problem 2.1: Given the nonlinear dynamical system (2) and a reach-avoid specification ϕ , compute (i) a ReLU NN architecture \mathcal{A} , (ii) an assignment of weights $\theta \in \Theta_{\mathcal{A}}$, and (iii) a set of initial states $\mathcal{X}_{\text{init}} \subseteq \mathcal{X}$, such that $\mathcal{NN}_{\theta}, \mathcal{X}_{\text{init}} \models \phi_{\text{safety}} \wedge \phi_{\text{liveness}}$.

III. FRAMEWORK

Before describing our approach to solve Problems 2.1, we start by recalling the connection between ReLU neural networks and Continuous Piece-Wise Affine (CPWA) functions as follows [32]:

Proposition 3.1: Every $\mathbb{R}^n \rightarrow \mathbb{R}^m$ ReLU NN represents a continuous piece-wise affine function.

In this paper, we confine our attention to CPWA controllers (and hence neural network controllers) that are selected from a bounded polytopic set $\mathcal{P}^K \times \mathcal{P}^b \subset \mathbb{R}^{m \times n} \times \mathbb{R}^m$, i.e., we assume that $K_i \in \mathcal{P}^K$ and $b_i \in \mathcal{P}^b$.

Our solution to Problem 2.1 is to use the mathematical model of the physical system (2) to guide the design of the NN architecture and bias its training. In particular, our approach is split into two components, one to address the safety specifications while the other one addresses the liveness specifications as described in the next two subsections.

A. Addressing Safety Specification ϕ_{safety}

Our approach to address the safety specifications ϕ_{safety} is as follows:

- **Step 1:** Capture the closed-loop behavior of the system under *all* CPWA controllers using an abstract model.

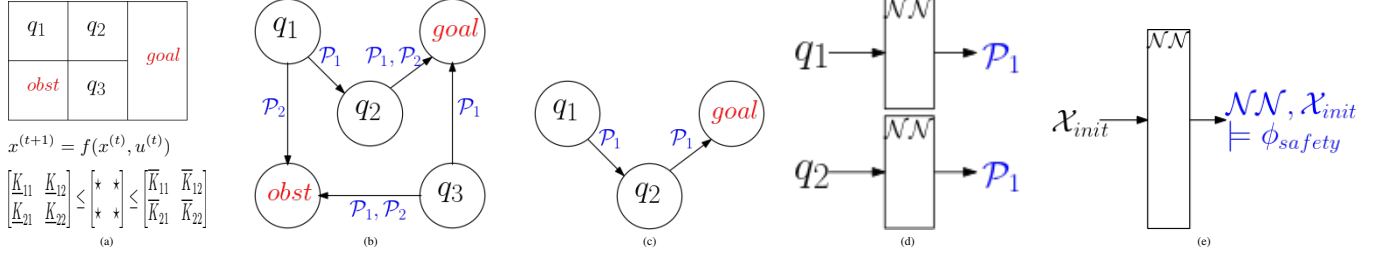


Fig. 1: (a) An example of a state space is partitioned into abstract states q_i , $i = 1, 2, 3$, and the controller parameter space is discretized into controller partitions \mathcal{P}_1 and \mathcal{P}_2 . (b) Posterior graph constructed using the dynamical model, the set of abstract states, and the set of controller partitions. (c) Assign one controller partition to each abstract state. Since both the controller partitions \mathcal{P}_1 and \mathcal{P}_2 are in the label from the state q_3 to the obstacle, q_3 is unsafe and hence is not considered in (c). (d) Train a local NN for each abstract state and enforce the CPWA functions represented by the NNs are within the assigned controller partitions. (e) Combine local NNs into a single NN controller that is guaranteed to satisfy the safety specification ϕ_{safety} .

Such abstract model can be obtained by extending current results on reachability analysis for polytopic systems [33].

- **Step 2:** Identify a subset of CPWA controllers that lead to correct behavior on the abstract model.
- **Step 3:** Design a NN architecture that matches the structure of the CPWA controllers that are identified to be correct.
- **Step 4:** Enforce the training of the NN to pick from the subset of the CPWA controllers that are identified to be correct.

Figure 1 conceptualizes our framework. To start with, we construct an abstract model by partitioning both the state space \mathcal{X} and the set of all allowed CPWA functions $\mathcal{P}^K \times \mathcal{P}^b$. In Figure 1 (b), the state space is partitioned into a set of abstract states $\mathbb{X} = \{q_1, q_2, q_3\}$ such that $q_i \subset \mathcal{X}$ and $\mathcal{X} = \bigcup_{i \in \{1,2,3\}} q_i$. Similarly, the controller space $\mathcal{P}^K \times \mathcal{P}^b$ is partitioned into a set of abstract controller partitions $\mathbb{P} = \{\mathcal{P}_1, \mathcal{P}_2\}$ such that $\mathcal{P}_i \in \mathcal{P}^K \times \mathcal{P}^b$ and $\mathcal{P}^K \times \mathcal{P}^b = \bigcup_{i \in \{1,2\}} \mathcal{P}_i$. The final abstract model is a non-deterministic finite transition system with nodes represent abstract states in \mathbb{X} and transitions are labeled by controller partitions in \mathbb{P} . Transitions between the abstract states are computed based on the reachable sets of the nonlinear system (2) from each abstract state and under every controller partition of the CPWA functions.

Based on the abstract model, we compute a function P_{safe} that maps each abstract state $q \in \mathbb{X}$ to a subset of the controller partitions (representing a collection of subsets of CPWA functions) that are considered to be safe at each abstract state. For example, in Figure 1 (b), since the transition from q_1 labeled by \mathcal{P}_2 leads to the obstacle, the controller partition \mathcal{P}_2 is unsafe at q_1 , and hence $P_{\text{safe}}(q_1) = \{\mathcal{P}_1\}$. Similarly, $P_{\text{safe}}(q_2) = \{\mathcal{P}_1, \mathcal{P}_2\}$. For the abstract state q_3 , since both \mathcal{P}_1 and \mathcal{P}_2 can lead to the obstacle, $P_{\text{safe}}(q_3)$ is empty, and hence q_3 is considered as an unsafe abstract state. The set of initial states that can provide safety guarantee is the union of the safe abstract states, i.e., $\mathcal{X}_{\text{init}} = q_1 \cup q_2$.

Using the set of safe controllers captured by $P_{\text{safe}}(q)$, it is direct to show that any neural network whose linear regions are aligned to the abstract states, and its weights are restricted to those in $P_{\text{safe}}(q)$ will always result into a NN that satisfies the

safety specifications. Therefore, we utilize this observation to construct a NN architecture that is guaranteed to be sufficient to implement a safe controller. Moreover, to ensure the safety of the resulting trained neural network, we propose a NN weight “projection” operator to enforce that the trained NN only gives rise to the CPWA functions indicated by $P_{\text{safe}}(q)$.

B. Addressing Liveness Specification ϕ_{liveness}

Our approach to addressing the liveness specification ϕ_{liveness} (reaching the goal) can be summarized as follows:

- **Step 1:** Use the abstract model to identify *candidate* controller partitions \mathcal{P}^* that can lead to satisfaction of the liveness properties.
- **Step 2:** Construct one local neural network NN_q for each of the abstract states. A sufficient architecture for this NN_q can be derived using ideas presented in [34].
- **Step 3:** Train the local neural networks NN_q using collected data. The data collection can be biased using the knowledge of \mathcal{P}^* to accelerate the process. We use the NN weight projection operator (discussed in the safety section) during training to ensure that the resulting NN still enjoys the safety specifications.
- **Step 4:** Combine all the local neural networks NN_q into a single global NN.

In the context of the example in Figure 1 (c), the controller partition \mathcal{P}_1 is assigned to both q_1 and q_2 as the *candidate* controller partition \mathcal{P}^* that *may* lead to the satisfaction of the liveness properties.

Next, we train one local neural network NN_q for each abstract state, or a subset of abstract states assigned with the same controller partition as shown in Figure 1 (d). During training of the local neural networks, we project the weights of the neural networks to enforce that the resulting NNs give rise to the CPWA functions belong to the assigned controller partition \mathcal{P}^* . Since the controller partition \mathcal{P}^* is chosen from the collection $P_{\text{safe}}(q)$, the resulting NN at q enjoys the same safety guarantees.

Finally, in Figure 1 (e), we combine the NNs trained for each abstract state into a single NN controller, by using layers with fixed weights to decide which part of the NN should be activated.

C. Formal Guarantees

We highlight that the proposed framework above *always* guarantees that the resulting NN satisfies the safety specification ϕ_{safety} thanks to the NN weight projection operator. This is reflected in Theorem 5.2 discussed in Section V-D.

On the other hand, achieving the liveness specification ϕ_{liveness} depends on the quality of the data used to train the neural networks and hence needs an extra step of formally verifying the resulting neural networks and iteratively change the candidate controller partition \mathcal{P}^* if needed. However, we argue that the resulting NN architecture is modular and is composed of a set of local networks NN_q that are more amenable to verification. The proposed architecture leads to a direct divide-and-conquer approach in which only local networks NN_q may need to be re-designed and trained whenever the liveness properties are not met.

IV. SAFE CONTROLLER PARTITION

In this section, we provide details on how to construct the abstract model that captures the behavior of all CPWA controllers along with how to choose the controller partitions that satisfy the specification ϕ .

A. Abstract Model

In order to capture the behavior of the system (2) under all possible CPWA controllers Ψ_{CPWA} , we construct a finite-state abstract model by discretizing both the state space and the set of all allowed CPWA functions. In particular, we partition the state space $\mathcal{X} \subset \mathbb{R}^n$ into a set of abstract states, denoted by $\mathbb{X} = \{q_1, \dots, q_N\}$, with each $q_i \in \mathbb{X}$ be an infinity-norm ball in \mathbb{R}^n . The goal region $\mathcal{X}_{\text{goal}} \subset \mathcal{X}$ is represented by a single abstract state $q_{\text{goal}} \in \mathbb{X}$, and the set of obstacles $\mathbb{X}_{\text{obst}} = \bigcup_{i=1}^o \{q_{\text{obst}_i}\}$ represents each obstacle $\mathcal{O}_i \subset \mathcal{X}$ by an abstract state $q_{\text{obst}_i} \in \mathbb{X}$, $i = 1, \dots, o$. Let $\text{Int}(q)$ denote the interior of a set q , then the partitioning satisfies $\mathcal{X} = \bigcup_{q \in \mathbb{X}} q$, and $\text{Int}(q_i) \cap \text{Int}(q_j) = \emptyset$ if $i \neq j$.

Similarly, we partition the controller space into polytopic sets. For simplicity of notation, we define the set of parameters $\mathcal{P}^{K \times b} \subset \mathbb{R}^{m \times (n+1)}$ be a polytope that combines \mathcal{P}^K and \mathcal{P}^b , and with some abuse of notation, we use $K_i(x)$ with a single parameter $K_i \in \mathcal{P}^{K \times b}$ to denote $K'_i x_i + b'_i$ with the pair $(K'_i, b'_i) = K_i$. The controller space $\mathcal{P}^{K \times b} \subset \mathbb{R}^{m \times (n+1)}$ is discretized into a set of polytopic sets in $\mathbb{R}^{m \times (n+1)}$, denoted by $\mathbb{P} = \{\mathcal{P}_1, \dots, \mathcal{P}_M\}$, such that $\mathcal{P}^{K \times b} = \bigcup_{\mathcal{P} \in \mathbb{P}} \mathcal{P}$, and $\text{Int}(\mathcal{P}_i) \cap \text{Int}(\mathcal{P}_j) = \emptyset$ if $i \neq j$. We call each of the subsets $\mathcal{P}_i \in \mathbb{P}$ a controller partition. Each controller partition $\mathcal{P} \in \mathbb{P}$ represents a subset of CPWA functions, by restricting parameters K_i in a CPWA function to take values from \mathcal{P} .

In order to reason about the safety property ϕ_{safety} , we introduce a posterior operator based on the dynamical model (2). The posterior of an abstract state $q \in \mathbb{X}$ under a controller partition $\mathcal{P} \in \mathbb{P}$ is the set of states that can be reached in one step from the states $x \in q$ by using an affine state feedback controller with parameters $K \in \mathcal{P}$, i.e.:

$$\text{Post}(q, \mathcal{P}) \triangleq \{f(x, K(x)) \in \mathbb{R}^n \mid x \in q, K \in \mathcal{P}\}. \quad (7)$$

A nonlinear system's posterior is often over-approximated in practice and we use $\overline{\text{Post}}$ to denote the corresponding operator.

Our abstract model is defined by using the set of abstract states \mathbb{X} , the set of controller partitions \mathbb{P} , and the posterior operator $\overline{\text{Post}}$. Intuitively, an abstract state $q \in \mathbb{X}$ has a transition to $q' \in \mathbb{X}$ under a controller partition $\mathcal{P} \in \mathbb{P}$ if the intersection between q' and $\overline{\text{Post}}(q, \mathcal{P})$ is non-empty.

Definition 4.1: (Posterior Graph) A posterior graph is a finite transition system $S_{\text{Post}} \triangleq (X, X_0, L, \longrightarrow)$, where:

- $X = \mathbb{X}$;
- $X_0 = \mathbb{X}$;
- $L = 2^{\mathbb{P}}$;
- $q \xrightarrow{l} q'$, if $q \notin \{q_{\text{goal}}\} \cup \mathbb{X}_{\text{obst}}$ and $l = \{\mathcal{P} \in \mathbb{P} \mid q' \cap \overline{\text{Post}}(q, \mathcal{P}) \neq \emptyset\} \neq \emptyset$.

Since the specification ϕ also requires reaching a goal region $\mathcal{X}_{\text{goal}} \subset \mathcal{X}$, we introduce a predecessor operator to capture the liveness property. The predecessor of an abstract state $q' \in \mathbb{X}$ under a controller partition $\mathcal{P} \in \mathbb{P}$ is defined as the set of states that can reach q' in one step by using an affine state feedback controller with some parameter $K \in \mathcal{P}$:

$$\text{Pre}(q', \mathcal{P}) \triangleq \{x \in \mathbb{R}^n \mid \exists K \in \mathcal{P} : f(x, K(x)) \in q'\}. \quad (8)$$

The computation of the posterior and the predecessor operators can be done by borrowing existing techniques in reachability analysis of polytopic systems [33], with some difference relies on the need to consider polytopic partitions of the parameter space $\mathcal{P}^{K \times b} \subset \mathbb{R}^{m \times (n+1)}$ instead of the well-studied problem of considering polytopic partitions of the input space $\mathcal{U} \subset \mathbb{R}^m$.

B. Computing Function P_{safe}

Once the abstract model is computed, our framework identifies a set of safe controller partitions $P_{\text{safe}}(q) \subseteq \mathbb{P}$ at each abstract state $q \in \mathbb{X}$. It is possible that the set $P_{\text{safe}}(q)$ is empty at some state $q \in \mathbb{X}$, in which case, the state q is considered to be unsafe.

To start with, we introduce an operator Next on the posterior graph S_{Post} . Given an arbitrary abstract state $q \in \mathbb{X}$ and a controller partition $\mathcal{P} \in \mathbb{P}$, the set $\text{Next}(q, \mathcal{P}) \subseteq \mathbb{X}$ consists of all abstract states that can be reached from q in one step, with the label of the corresponding transition in S_{Post} contains \mathcal{P} :

$$\text{Next}(q, \mathcal{P}) \triangleq \{q' \in \mathbb{X} \mid q' \cap \overline{\text{Post}}(q, \mathcal{P}) \neq \emptyset\}. \quad (9)$$

Similar to standard reachability analysis, a state $q \in \mathbb{X}$ is considered to be safe if the posteriors computed in multiple steps do not intersect the obstacles. Unique to our problem, the parameter space $\mathcal{P}^{K \times b} \subset \mathbb{R}^{m \times (n+1)}$ is discretized into a set of controller partitions \mathbb{P} , and at each state $q \in \mathbb{X}$, it has the freedom to choose one of the controller partitions $\mathcal{P} \in \mathbb{P}$ when computing the posterior. To capture this freedom in the choice of controller partitions, we identify a series of unsafe sets in a recursive manner by backtracking from the set of obstacles \mathbb{X}_{obst} in the posterior graph S_{Post} :

$$\begin{aligned} \mathbb{X}_{\text{unsafe}}^0 &= \mathbb{X}_{\text{obst}} \\ \mathbb{X}_{\text{unsafe}}^1 &= \{q \in \mathbb{X} \mid \forall \mathcal{P} \in \mathbb{P} : \text{Next}(q, \mathcal{P}) \cap \mathbb{X}_{\text{unsafe}}^0 \neq \emptyset\} \cup \mathbb{X}_{\text{unsafe}}^0 \\ &\vdots \\ \mathbb{X}_{\text{unsafe}}^k &= \{q \in \mathbb{X} \mid \forall \mathcal{P} \in \mathbb{P} : \text{Next}(q, \mathcal{P}) \cap \mathbb{X}_{\text{unsafe}}^{k-1} \neq \emptyset\} \cup \mathbb{X}_{\text{unsafe}}^{k-1} \end{aligned}$$

The backtracking stops when it does not find new unsafe states, i.e., $\mathbb{X}_{\text{unsafe}}^k = \mathbb{X}_{\text{unsafe}}^{k-1}$. Intuitively, the set of unsafe states $\mathbb{X}_{\text{unsafe}}^k$ consists of abstract states that cannot avoid reaching the obstacles by choosing controller partitions from \mathbb{P} .

Then, the set of safe states \mathbb{X}_{safe} consists of all the states that can avoid transition to the set $\mathbb{X}_{\text{unsafe}}^k$:

$$\mathbb{X}_{\text{safe}} \triangleq \{q_0 \in \mathbb{X} \setminus \mathbb{X}_{\text{unsafe}}^k \mid \exists \mathcal{P} \in \mathbb{P} : \text{Next}(q_0, \mathcal{P}) \cap \mathbb{X}_{\text{unsafe}}^k = \emptyset\}. \quad (10)$$

Correspondingly, the function P_{safe} maps each abstract state $q_0 \in \mathbb{X}_{\text{safe}}$ to a subset of controller partitions that can be used to avoid transition to $\mathbb{X}_{\text{unsafe}}^k$:

$$P_{\text{safe}} : q_0 \mapsto \{\mathcal{P}_0 \in \mathbb{P} \mid \text{Next}(q_0, \mathcal{P}_0) \cap \mathbb{X}_{\text{unsafe}}^k = \emptyset\}. \quad (11)$$

The following theorem summarizes the safety property:

Theorem 4.2: Let $\Psi_{q, \text{CPWA}}$ be a state feedback CPWA controller (as defined in (1)) corresponding to an abstract state $q \in \mathbb{X}_{\text{safe}}$ with arbitrarily chosen parameter K_i that satisfy $K_i \in \mathcal{P}$ and $\mathcal{P} \in P_{\text{safe}}(q)$. Consider a feedback controller Ψ constructed as follows:

$$\Psi(x) = \Psi_{q, \text{CPWA}}(x) \quad \forall x \in q, \quad \forall q \in \mathbb{X}_{\text{safe}}.$$

Then, with the set of initial states $\mathcal{X}_{\text{init}} = \bigcup_{q \in \mathbb{X}_{\text{safe}}} q$, the system (2) controlled by Ψ satisfies the safety specification ϕ_{safety} , i.e., $\Psi, \mathcal{X}_{\text{init}} \models \phi_{\text{safety}}$.

By Theorem 4.2, the system is guaranteed to satisfy the safety specification ϕ_{safety} by applying any CPWA controller $\Psi_{q, \text{CPWA}}$ at each abstract state $q \in \mathbb{X}_{\text{safe}}$, as long as the controller parameters K_i are chosen from the safe controller partitions $\mathcal{P} \in P_{\text{safe}}(q)$. This allows us to conclude the safety guarantee provided by a NN controller if the CPWA functions represented by the NN are chosen from the safe controller partitions, as we show in detail in Section IV-D.

Proof: When the backtracking stops, for every abstract state $q_0 \in \mathbb{X} \setminus \mathbb{X}_{\text{unsafe}}^k$, there exists a controller partition $\mathcal{P}_0 \in \mathbb{P}$ such that $\text{Next}(q_0, \mathcal{P}_0) \cap \mathbb{X}_{\text{unsafe}}^k = \emptyset$. By (10), $\mathbb{X}_{\text{safe}} = \mathbb{X} \setminus \mathbb{X}_{\text{unsafe}}^k$. Then, by (11), for every state $q_0 \in \mathbb{X}_{\text{safe}}$, and any partition $\mathcal{P}_0 \in P_{\text{safe}}(q_0)$, $\text{Next}(q_0, \mathcal{P}_0) \subseteq \mathbb{X}_{\text{safe}}$. Therefore, by applying an arbitrary controller partition $\mathcal{P}_0 \in P_{\text{safe}}(q_0)$ at $q_0 \in \mathbb{X}_{\text{safe}}$, none of the resulting trajectories in the posterior graph S_{Post} can reach an obstacle state $q_{\text{obst}} \in \mathbb{X}_{\text{obst}}$. By the construction of posterior graph S_{Post} , the safety property provided by $\mathcal{P} \in P_{\text{safe}}(q)$ remain holds for any CPWA controller with parameters $K_i \in \mathcal{P}$.

C. Sufficient NN Architecture for Safety Specifications

Once the set of safe abstract states \mathbb{X}_{safe} and the associated map P_{safe} is identified, the next step is to construct a neural network architecture that is sufficient to implement a safe controller. This NN will be augmented in Section V to account for the liveness properties as well. The following lemma identifies a sufficient number of linear regions needed by any piece-wise affine function to satisfy the safety property ϕ_{safety} . In Section V-D, this number is transformed into a NN architecture that is guaranteed to respect the sufficient number of linear regions needed for the safety guarantees.

Lemma 4.3: There is a piece-wise affine function $\Psi : \mathcal{X} \rightarrow \mathcal{U}$ with the number of linear regions be $|\mathbb{X}_{\text{safe}}|$, such that the system (2) controlled by Ψ satisfies the safety property ϕ_{safety} .

Proof: By Theorem 4.2, the safety property is satisfied by applying any CPWA function with $K_i \in \mathcal{P}$ and $\mathcal{P} \in P_{\text{safe}}(q)$. In particular, we consider the parameter K_i is fixed at q , i.e., each abstract state $q \in \mathbb{X}_{\text{safe}}$ is a linear region. Then, the sufficient number of linear regions is same as the number of states in \mathbb{X}_{safe} .

D. Safe Training Using NN Weight Projection

As described in Section III, the final NN consists of several local networks NN_q that will be trained to account for the liveness property. Nevertheless, to ensure that the safety property is met by each of the local networks NN_q , we propose a NN weight projection operator that can be incorporated in the training of these local NNs. This operator projects the weights of each NN_q to ensure that the network gives rise to the CPWA functions that belong to the controller partitions $\mathcal{P}^* \in P_{\text{safe}}(q)$ (the selection of \mathcal{P}^* based on the liveness property is presented in Section V-A).

To that end, we recall that every local network NN_q represents a CPWA function \mathcal{NN}_θ that partitions the state space into a set of linear regions $\mathbb{L}_{\mathcal{NN}_\theta} = \{\mathcal{R}_1, \dots, \mathcal{R}_L\}$, with an affine function parametrized by $K_i \in \mathbb{R}^{m \times (n+1)}$ associated to each linear region \mathcal{R}_i , $i = 1, \dots, L$. During the projection phase, our algorithm identifies the subset of linear regions that intersect with the abstract state q for which the NN is trained:

$$\mathbb{L}_{\mathcal{NN}_\theta \cap q} \triangleq \{\mathcal{R} \in \mathbb{L}_{\mathcal{NN}_\theta} \mid q \cap \mathcal{R} \neq \emptyset\}. \quad (12)$$

Then, for each affine function with parameter K_i at region $\mathcal{R}_i \in \mathbb{L}_{\mathcal{NN}_\theta \cap q}$, our approach enforces $K_i \in \mathcal{P}^*$ by adjusting the weights of the trained NN.

The projection of NN_q weights can be done by solving a convex optimization problem. Consider a K -layer NN with currently trained weights $\hat{\theta} = (\hat{\theta}^{(1)}, \dots, \hat{\theta}^{(K)})$, where we use the hat notation for weights that are given by any training procedure. As a common practice, we consider there is no ReLU activation function in the output layer of the NN, and hence the subset of intersected regions $\mathbb{L}_{\mathcal{NN}_\theta \cap q} \subseteq \mathbb{L}_{\mathcal{NN}_{\hat{\theta}}}$ only depends on the hidden layer weights $\hat{\theta}^{(l)}$, $l = 1, \dots, K-1$. During projection, our algorithm adjusts the output layer weights $\theta^{(K)}$ by minimizing its difference from the currently trained weights $\hat{\theta}^{(K)}$. By fixing the hidden layer weights as given by the training, the subset of intersected regions $\mathbb{L}_{\mathcal{NN}_{\hat{\theta}} \cap q}$ can be determined. Controller parameters K_i corresponding to linear regions $\mathcal{R}_i \in \mathbb{L}_{\mathcal{NN}_{\hat{\theta}} \cap q}$ are brought into the controller partition \mathcal{P}^* by solving the following quadratic program:

$$\begin{aligned} \min_{\theta^{(K)}} & \|\theta^{(K)} - \hat{\theta}^{(K)}\| \\ \text{s.t.} & K_i \in \mathcal{P}^*, \quad \forall \mathcal{R}_i \in \mathbb{L}_{\mathcal{NN}_{\hat{\theta}} \cap q}. \end{aligned} \quad (13)$$

The weights $\theta^{(K)}$ solved from (13) are then used to replace the currently trained output layer weights $\hat{\theta}^{(K)}$. These two processes, i.e., training and projection, can be done either in an alternating way, or only projecting once at the end of training. In the result section, we show that the trained NNs perform well even with just a single projection at the end. Notice that the optimization problem (13) could be infeasible, which can be resolved by improving the hidden layer weights with more training effort.

Example: We illustrate the optimization problem (13) by a toy example. Consider a neural network $\mathcal{NN}_\theta : \mathbb{R}^2 \rightarrow \mathbb{R}$ has a single hidden layer with two neurons: $h_1 = \max\{0, W_{11}^{(1)}x_1 + W_{12}^{(1)}x_2\}$, $h_2 = \max\{0, W_{21}^{(1)}x_1 + W_{22}^{(1)}x_2\}$, and the output layer $u = W_{11}^{(2)}h_1 + W_{12}^{(2)}h_2$. Based on the activation pattern of the two hidden layer neurons, the NN has four linear regions $\mathcal{R}_1, \dots, \mathcal{R}_4$, and the corresponding CPWA function \mathcal{NN}_θ can be written as:

$$\mathcal{NN}_\theta(x) = \begin{cases} (W_{11}^{(1)}W_{11}^{(2)} + W_{21}^{(1)}W_{12}^{(2)})x_1 + (W_{12}^{(1)}W_{11}^{(2)} + W_{22}^{(1)}W_{12}^{(2)})x_2, & \text{if } x \in \mathcal{R}_1 \\ W_{11}^{(1)}W_{11}^{(2)}x_1 + W_{12}^{(1)}W_{11}^{(2)}x_2, & \text{if } x \in \mathcal{R}_2 \\ W_{21}^{(1)}W_{12}^{(2)}x_1 + W_{22}^{(1)}W_{12}^{(2)}x_2, & \text{if } x \in \mathcal{R}_3 \\ 0, & \text{if } x \in \mathcal{R}_4 \end{cases}$$

Consider the controller partition \mathcal{P}^* is given by $K_1 \in [K_1^{\text{low}}, K_1^{\text{up}}]$ and $K_2 \in [K_2^{\text{low}}, K_2^{\text{up}}]$. Suppose the abstract state q intersects \mathcal{R}_1 and \mathcal{R}_2 , then problem (13) can be written as:

$$\begin{aligned} \min_{W_{11}^{(2)}, W_{12}^{(2)}} & (W_{11}^{(2)} - \widehat{W}_{11}^{(2)})^2 + (W_{12}^{(2)} - \widehat{W}_{12}^{(2)})^2 \\ \text{s.t.} & \widehat{W}_{11}^{(1)}W_{11}^{(2)} + \widehat{W}_{21}^{(1)}W_{12}^{(2)} \in [K_1^{\text{low}}, K_1^{\text{up}}], \\ & \widehat{W}_{11}^{(1)}W_{11}^{(2)} \in [K_1^{\text{low}}, K_1^{\text{up}}], \\ & \widehat{W}_{12}^{(1)}W_{11}^{(2)} + \widehat{W}_{22}^{(1)}W_{12}^{(2)} \in [K_2^{\text{low}}, K_2^{\text{up}}], \\ & \widehat{W}_{12}^{(1)}W_{11}^{(2)} \in [K_2^{\text{low}}, K_2^{\text{up}}] \end{aligned}$$

Since all the hidden layer weights $\widehat{W}_{ij}^{(1)}$ are fixed as given by the training, it yields a quadratic program.

The following result shows the safety guarantee provided by projecting weights during training:

Theorem 4.4: Given an abstract state $q \in \mathbb{X}_{\text{safe}}$ and an arbitrary controller partition $\mathcal{P}^* \in P_{\text{safe}}(q)$. Let the weight assignment θ of NN_q be computed by (13), then the resulting $\text{NN}_q = \mathcal{NN}_\theta$ is guaranteed to be safe at q , i.e., $\text{NN}_q, q \models \phi_{\text{safety}}$.

Proof: Notice that the subset of intersected regions $\mathbb{L}_{\mathcal{NN}_\theta}$ only depends on the hidden layer weights, which remain unchanged during the projection. Then, the constraints in problem (13) along with Theorem 4.2 directly leads to the result.

V. EXTENSION TO LIVENESS PROPERTY

A. Controller Partition Assignment

Among all the safe controller partitions in $P_{\text{safe}}(q)$, we assign one of them $\mathcal{P}^* \in P_{\text{safe}}(q)$ to each abstract state $q \in \mathbb{X}_{\text{safe}}$, by taking into account the liveness specification ϕ_{liveness} . The liveness property requires that the nonlinear system (2) can reach the goal $\mathcal{X}_{\text{goal}} \subset \mathcal{X}$ by using the trained NN controller. Unlike the safety property which can be enforced using the projection operator, achieving the liveness property depends on practical issues, such as the amount of training data and the effort spent on training the NNs. To that end, we show that the safety guarantee provided by our algorithm does not impede the collection of training data, and hence the NNs can be trained to satisfy the liveness property by using standard learning techniques.

Since the posterior graph S_{Post} over-approximates the behavior of the system, a transition from q to q' under \mathcal{P} does not guarantee every state $x \in q$ can reach q' in one step, by applying input $u = K(x)$ with parameter $K \in \mathcal{P}$. To

capture the liveness property, we introduce the predecessor graph based on the predecessor operator given in Section IV-A:

Definition 5.1: (Predecessor Graph) A predecessor graph is a finite transition system $S_{\text{Pre}} \triangleq (X, X_0, L, \rightarrow)$, where:

- $X = \mathbb{X}_{\text{safe}} \cup \{q_{\text{goal}}\}$;
- $X_0 = \mathbb{X}_{\text{safe}}$;
- $L = 2^{\mathbb{P}}$;
- $q \xrightarrow{l} q'$, if $q \neq q_{\text{goal}}$ and $l = \{\mathcal{P} \in P_{\text{safe}}(q) \mid q \cap \text{Pre}(q', \mathcal{P}) \neq \emptyset\} \neq \emptyset$.

Notice that in the construction of S_{Pre} , we restrict transition labels to the safe controller partitions $\mathcal{P} \in P_{\text{safe}}(q)$ at each state $q \in \mathbb{X}_{\text{safe}}$. Let \mathcal{T}_{Pre} be the set of all trajectories over the predecessor graph S_{Pre} , then we use $\pi_X^{(t)} : \omega \mapsto q$ to denote the map from a trajectory $\omega \in \mathcal{T}_{\text{Pre}}$ to the abstract state q at time step t , and use $\pi_L^{(t)} : \omega \mapsto l$ to denote the map from $\omega \in \mathcal{T}_{\text{Pre}}$ to the label $l \in 2^{\mathbb{P}}$ associated to the transition from $\pi_X^{(t)}(\omega)$ to $\pi_X^{(t+1)}(\omega)$. By extending the formulation of specification to the abstract state space, a trajectory ω in S_{Pre} satisfies the reach-avoid specification ϕ , denoted by $\omega \models \phi$, if ω reaches the goal state q_{goal} in T steps. Similar to the notation introduced for the posterior graph, let $\text{Next}(q, \mathcal{P})$ be the set of states that can be reached from q under the partition \mathcal{P} in one step:

$$\text{Next}(q, \mathcal{P}) \triangleq \{q' \in \mathbb{X}_{\text{safe}} \cup \{q_{\text{goal}}\} \mid q \cap \text{Pre}(q', \mathcal{P}) \neq \emptyset\}. \quad (14)$$

At each state $q \in \mathbb{X}_{\text{safe}}$, our objective is to choose the candidate controller partition $\mathcal{P}^* \in P_{\text{safe}}(q)$ that can lead most of the states $x \in q$ to the goal. To that end, we restrict our attention to trajectories in S_{Pre} that progress towards the goal. That is, let $|\omega|$ be the length of a trajectory $\omega \in \mathcal{T}_{\text{Pre}}$, and $\text{Dist} : \mathbb{X}_{\text{safe}} \rightarrow \mathbb{N}$ map a state $q \in \mathbb{X}_{\text{safe}}$ to the length of the shortest trajectory from the state q to the goal in the predecessor graph S_{Pre} . Then, we use $\mathcal{T}'_{\text{Pre}} \subseteq \mathcal{T}_{\text{Pre}}$ to denote the subset of trajectories that lead to the goal:

$$\begin{aligned} \mathcal{T}'_{\text{Pre}} & \triangleq \{\omega \in \mathcal{T}_{\text{Pre}} \mid \text{Dist}(\pi_X^{(t)}(\omega)) < \text{Dist}(\pi_X^{(t-1)}(\omega)), \\ & t = 1, \dots, |\omega| - 1\}. \end{aligned} \quad (15)$$

Now we can define the subset of abstract states that progress towards the goal, denoted by $\mathcal{Q}_{q, \mathcal{P}} \subseteq \text{Next}(q, \mathcal{P})$, as the set of abstract states along a trajectory $\omega \in \mathcal{T}'_{\text{Pre}}$ that satisfies the given specification:

$$\begin{aligned} \mathcal{Q}_{q, \mathcal{P}} & \triangleq \{q' \in \text{Next}(q, \mathcal{P}) \mid \exists \omega \in \mathcal{T}'_{\text{Pre}} : \omega \models \phi, \\ & \pi_X^{(0)}(\omega) = q, \pi_X^{(1)}(\omega) = q', \mathcal{P} \in \pi_L^{(0)}(\omega)\}. \end{aligned} \quad (16)$$

Then, the intersection between the state q and the predecessors of $q' \in \mathcal{Q}_{q, \mathcal{P}}$ under the controller partition \mathcal{P} is given by:

$$\mathcal{I}_{q, \mathcal{P}} \triangleq \bigcup_{q' \in \mathcal{Q}_{q, \mathcal{P}}} (q \cap \text{Pre}(q', \mathcal{P})). \quad (17)$$

Intuitively, the set $\mathcal{I}_{q, \mathcal{P}}$ measures the portion of states $x \in q$ that can reach the goal by applying input $u = K(x)$ with $K \in \mathcal{P}$ at the first step. Then, our algorithm assigns a state $q \in \mathbb{X}_{\text{safe}}$ with the controller partition $\mathcal{P}^* \in P_{\text{safe}}(q)$ that corresponds to the largest set $\mathcal{I}_{q, \mathcal{P}^*}$ among all the sets $\mathcal{I}_{q, \mathcal{P}}$ for $\mathcal{P} \in P_{\text{safe}}(q)$. Indeed, and as mentioned in Section III, such procedure only ranks the available choices of controller partitions and one may need to iterate over the remaining choices using the same heuristic above.

B. Selecting Architecture for Local NNs

Given the assigned controller partition $\mathcal{P}^* \in P_{\text{safe}}(q)$ at each state $q \in \mathbb{X}_{\text{safe}}$, the next step is to select a NN architecture (number of layers and number of neurons per layer) for each of the local networks NN_q . Such an architecture, should be sufficient to implement any CPWA function within the selected controller partition $\mathcal{P}^* \in P_{\text{safe}}(q)$.

Unfortunately, such neural network architecture may not exist without additional assumptions on the controllability of the underlying system, e.g., the existence of a Lipschitz continuous controller that satisfy the specification ϕ_{liveness} [34]. We note that the current definition of the predecessor operator Pre can be slightly modified to ensure the existence of such Lipschitz continuous controllers, thanks to the fact that \mathcal{P}^* represents a set of CPWA functions which are by definition Lipschitz continuous. For sake of brevity and due to space constraints, we omit this discussion as it follows similar arguments as the one detailed in [34]. Finally, we refer to such architecture as $\mathcal{A}_{q, \mathcal{P}^*}$.

C. Data Collection and Training of Local NNs

For training of the local networks NN_q , we consider the training data are either already available or need to be collected by invoking an expert. In the first scenario, unlike most learning algorithms that can directly use the available data, our approach needs to take into account the abstract states and controller partitions associated with the data. In case training data are not available, we assume to have access to an expert for collecting data, with extra consideration that the collected data need be aligned with the controller partition assignment.

We consider the collection of training data takes the form of $\{(x, u)\}$, where each state $x \in \mathcal{X}$ is associated with an input label $u \in \mathbb{R}^m$. Given a collection of data \mathcal{D} from trajectories that satisfy the given specification, Algorithm 1 selects a subset of data $\mathcal{D}_q \subseteq \mathcal{D}$ used for training the local network NN_q at q , without the need to compute predecessors or invoke an expert. Specifically, for each data point $(x, u) \in \mathcal{D}$, it determines the corresponding controller partition $\mathcal{P} \in P_{\text{safe}}(q)$ by solving a linear feasibility problem, under the constraints $u = K(x)$, $K \in \mathcal{P}$ (one data point (x, u) may correspond to multiple partitions \mathcal{P}) (line 7 in Algorithm 1). After classifying a subset of data $\mathcal{D}_{q, \mathcal{P}}$ associated to each controller partition \mathcal{P} , the algorithm selects $\mathcal{P}^* \in P_{\text{safe}}(q)$ that corresponds to the most amount of available data points (line 9-13 in Algorithm 1).

By assuming having access to an expert, Algorithm 2 collects training data that are consistent with the assigned controller partitions. It first computes the intersection between the state q and the predecessors of states $q' \in \mathcal{Q}_{q, \mathcal{P}}$ (line 2-8 in Algorithm 2). Then, the algorithm selects $\mathcal{P}^* \in P_{\text{safe}}(q)$ corresponding to the largest intersection with the predecessors (line 9-12 in Algorithm 2). With access to an expert, it samples states $x \in q$ and synthesizes one step transition to reach abstract states in $\mathcal{Q}_{q, \mathcal{P}^*}$, by using an affine controller with parameter $K \in \mathcal{P}^*$ (line 13-15 in Algorithm 2).

With the collection of training data \mathcal{D}_q that are aligned with the controller partition assignment $\mathcal{P}^* \in P_{\text{safe}}(q)$ at each abstract state $q \in \mathbb{X}_{\text{safe}}$, the local NNs can be trained

to satisfy the liveness specification ϕ_{liveness} , along with the safety guarantee enforced by projecting weights at the end of training.

Algorithm 1 CLASSIFY-DATA ($q, P_{\text{safe}}(q), \mathcal{D}$)

```

1:  $\mathcal{D}_q = \text{list}()$ ,  $\mathcal{P}^* = \text{None}$ , current = 0
2: for  $\mathcal{P} \in P_{\text{safe}}(q)$  do
3:    $\mathcal{D}_{q, \mathcal{P}} = \text{list}()$ 
4:   for  $(x, u) \in \mathcal{D}$  do
5:     if  $x \in q$  then
6:       for  $\mathcal{P} \in P_{\text{safe}}(q)$  do
7:         if  $u = K(x)$ ,  $K \in \mathcal{P}$  then
8:            $\mathcal{D}_{q, \mathcal{P}}.\text{append}((x, u))$ 
9:   for  $\mathcal{P} \in P_{\text{safe}}(q)$  do
10:    if  $|\mathcal{D}_{q, \mathcal{P}}| > \text{current}$  then
11:      current =  $|\mathcal{D}_{q, \mathcal{P}}|$ 
12:       $\mathcal{D}_q = \mathcal{D}_{q, \mathcal{P}}$ 
13:       $\mathcal{P}^* = \mathcal{P}$ 
14: Return  $\mathcal{D}_q, \mathcal{P}^*$ 

```

Algorithm 2 COLLECT-DATA ($q, P_{\text{safe}}(q), S_{\text{Pre}}$)

```

1:  $\mathcal{D}_q = \text{list}()$ ,  $\mathcal{P}^* = \text{None}$ , current = 0
2: for  $\mathcal{P} \in P_{\text{safe}}(q)$  do
3:    $\mathcal{I}_{q, \mathcal{P}} = \text{set}()$ ,  $\mathcal{Q}_{q, \mathcal{P}} = \text{set}()$ 
4:   for  $q' \in \text{Next}(q, \mathcal{P})$  do
5:     if  $\exists \omega \in \mathcal{T}'_{\text{Pre}}: \omega \models \phi$ ,  $\pi_X^{(0)}(\omega) = q$ ,  $\pi_X^{(1)}(\omega) = q'$ ,  $\mathcal{P} \in \pi_L^{(0)}(\omega)$  then
6:        $\text{isect} = q \cap \text{Pre}(q', \mathcal{P})$ 
7:        $\mathcal{I}_{q, \mathcal{P}} = \mathcal{I}_{q, \mathcal{P}} \cup \text{isect}$ 
8:        $\mathcal{Q}_{q, \mathcal{P}} = \mathcal{Q}_{q, \mathcal{P}} \cup \{q'\}$ 
9:   for  $\mathcal{P} \in P_{\text{safe}}(q)$  do
10:    if  $\text{size}(\mathcal{I}_{q, \mathcal{P}}) > \text{current}$  then
11:       $\mathcal{P}^* = \mathcal{P}$ 
12:      current =  $\text{size}(\mathcal{I}_{q, \mathcal{P}})$ 
13:   for sample  $x \in q$  do
14:      $u = \text{expert}(x, \mathcal{P}^*, \mathcal{Q}_{q, \mathcal{P}^*})$ 
15:      $\mathcal{D}_q.\text{append}((x, u))$ 
16: Return  $\mathcal{D}_q, \mathcal{P}^*$ 

```

D. Combined NN Controller

The final step of our framework is to combine all the local networks NN_q into one global NN controller. Figure 2 (a) shows the overall structure of the global NN controller obtained by combining modules $[\text{NN}_q]_M$ that correspond to the local networks NN_q . As input to the NN controller, the state $x \in \mathcal{X}$ is fed into all the local networks, and the output of the NN controller is the summation of all the local network outputs. In the figure, we show a single output for simplicity, but it can be easily extended to multiple outputs (indeed, even in the figures, u and u_q can be thought as vectors in \mathbb{R}^m , and the summation and product operations correspond to vector addition and scalar multiplication, respectively).

Each module $[\text{NN}_q]_M$ consists of two parts: logic and ReLU NN. The logic component decides whether the current state x is in the abstract state q associated with $[\text{NN}_q]_M$, and outputs 1 if the answer is affirmative, 0 otherwise. The ReLU NN is the neural network trained for this abstract state q . By multiplying the outputs of the logic and the ReLU NN, output of the module $[\text{NN}_q]_M$ is identical to the output of the ReLU NN

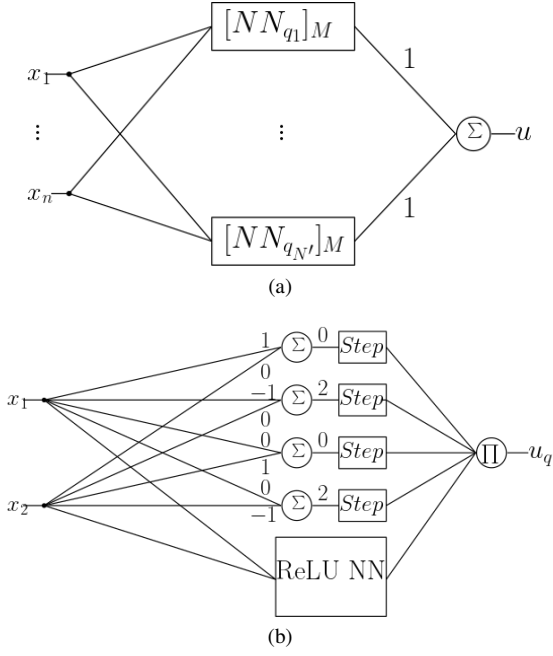


Fig. 2: (a) The combined NN controller consists of one module $[\text{NN}_{q_i}]_M$ for each abstract state $q_i \in \mathbb{X}_{\text{safe}}$, where $N' = |\mathbb{X}_{\text{safe}}|$. (b) An example of the module $[\text{NN}_q]_M$, where the state $q \subset \mathbb{R}^2$ is given by $q = [0, 2] \times [0, 2]$.

if $x \in q$, and zero otherwise. Figure 2 (b) is an example of the module $[\text{NN}_q]_M$, where we choose an arbitrary abstract state $q \subset \mathbb{R}^2$ given by $0 \leq x_1 \leq 2$ and $0 \leq x_2 \leq 2$.

The logic component in each module $[\text{NN}_q]_M$ can be implemented as a single layer NN with fixed weights. Given the H -representation $Ax \leq c$ of the state q , the weight matrix and the bias vector associated to the single layer NN are $W^{(1)} = -A$ and $b^{(1)} = c$, respectively. Essentially, this choice of weights encodes one hyperplane inequality in the H -representation to each neuron in the single layer. To represent whether an inequality holds, we use a step function as the nonlinear activation function for the single layer:

$$\text{Step}(x) = \begin{cases} 1 & \text{if } x \geq 0 \\ 0 & \text{otherwise.} \end{cases} \quad (18)$$

The product of the outputs of all the neurons in the single layer is computed at the end (by the product operator Π), and hence the logic component returns 1 if and only if all the hyperplane inequalities are satisfied. We refer to the architecture of the logic component as $\mathcal{A}_{q,\Pi}$ and the architecture of the whole module $[\text{NN}_q]_M$ as $\mathcal{A}_q = [\mathcal{A}_{q,\mathcal{P}^*} \parallel \mathcal{A}_{q,\Pi}]$, where \parallel denotes the parallel composition of the ReLU NN and the logic component. Using the same notation, we can define the architecture of the global NN as follows:

$$\mathcal{A} = \mathcal{A}_{q_1} \parallel \dots \parallel \mathcal{A}_{q_{N'}}.$$

Now the guarantees of the combined NN controller can be summarized as follows whose proof follows directly from the discussion above along with Theorem 4.2, Lemma 4.3, and Theorem 4.4:

Theorem 5.2: Consider the nonlinear system (2) and the reach-avoid specification $\phi = \phi_{\text{safety}} \wedge \phi_{\text{liveness}}$. Let the controller partition assignment $\mathcal{P}_1^*, \dots, \mathcal{P}_{N'}^*$ and the local neural networks $\text{NN}_{q_1}, \dots, \text{NN}_{q_{N'}}$ satisfy the following conditions:

- the assignment \mathcal{P}_i^* satisfies $\mathcal{P}_i^* \in P_{\text{safe}}(q_i)$,
- the NN architecture \mathcal{A}_{q_i} satisfies $\mathcal{A}_{q_i} = [\mathcal{A}_{q_i,\mathcal{P}^*} \parallel \mathcal{A}_{q_i,\Pi}]$,
- the NN weights θ_i of NN_{q_i} is projected on \mathcal{P}_i^* using the projection operator (13).

Then, the neural network NN with architecture $\mathcal{A} = \mathcal{A}_{q_1} \parallel \dots \parallel \mathcal{A}_{q_{N'}}$ and local networks $\text{NN}_{q_1}, \dots, \text{NN}_{q_{N'}}$ satisfies $\text{NN}, \mathcal{X}_{\text{init}} \models \phi_{\text{safety}}$ with $\mathcal{X}_{\text{init}} = \bigcup_{q \in \mathbb{X}_{\text{safe}}} q$. Moreover, if all the local networks NN_{q_i} satisfy:

$$\text{Reach}(q_i, \text{NN}_{q_i}) \subseteq \bigcup_{q' \in \mathcal{Q}_{q_i, \mathcal{P}_i^*}} q', \quad (19)$$

where $\mathcal{Q}_{q_i, \mathcal{P}_i^*}$ is defined as (16) and $\text{Reach}(q, \text{NN}_q)$ is defined as:

$$\text{Reach}(q, \text{NN}_q) \triangleq \{f(x, \text{NN}_q(x)) \mid x \in q\}, \quad (20)$$

then:

$$\text{NN}, \mathcal{X}_{\text{init}} \models \phi_{\text{liveness}}.$$

In words, Theorem 5.2 guarantees that any global NN composed from provably safe local networks is still safe (i.e., satisfy ϕ_{safety}). This is a reflection of the fact that the composition of the global network respects the linear regions on which the local networks are defined. Moreover, if each of the local NNs satisfies the *local* reachability property in (19), then the global NN satisfies the liveness property ϕ_{liveness} . This is a reflection of the fact that the set $\mathcal{Q}_{q,\mathcal{P}}$ in (16) is defined to guarantee progress towards the goal.

In practice, by combining the local NNs into a single controller, it allows one to repair the NN controller in a systematic way when it fails to meet the local liveness property (19). Specifically, with the observation that the behavior of the system is not as expected at a certain abstract state $q \in \mathbb{X}_{\text{safe}}$, only the local neural network NN_q need to be improved, such as by further training with augmented data collected at the state q , without affecting NNs that satisfy the specification at other abstract states.

VI. EXPERIMENTAL RESULTS

We implemented the proposed framework and evaluated both the resulting control performance and the scalability of the proposed algorithm. We used TIRA [35] to compute the reachable sets and FORCES [36], [37] to collect training data as shown in line 14 of Algorithm 2. All experiments were executed on an Intel Core i9 2.4-GHz processor with 32 GB of memory.

A. Controller Performance Comparison: Provably Correct NN Controllers vs Standard Training Techniques

We first present trajectories of a wheeled robot under the control of NN controllers trained by our algorithm. Let the state vector of the system be $x = [\zeta_x, \zeta_y, \theta]^T \in \mathcal{X} \subset \mathbb{R}^3$, where ζ_x, ζ_y denote the coordinates of the robot, and θ is the

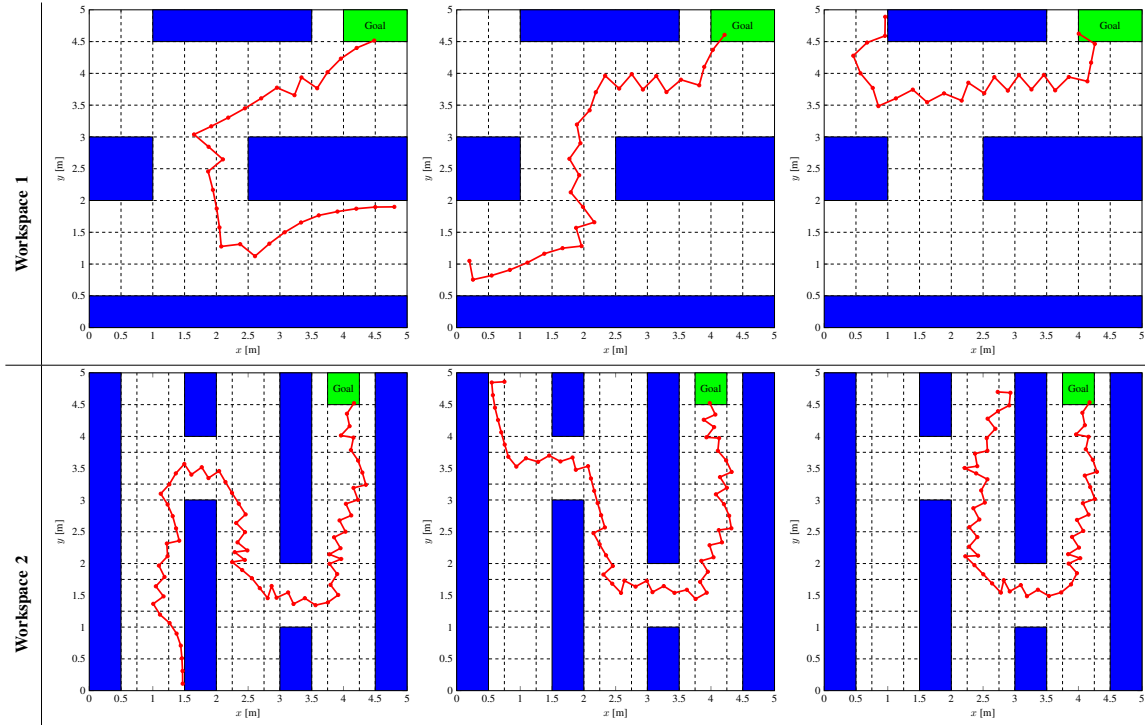


Fig. 3: Workspace 1 (the upper row) and workspace 2 (the lower row) are partitioned into abstract states (dash lines) either uniformly or non-uniformly. Trajectories starting from different initial states satisfy both the safety specification ϕ_{safety} (blue areas are obstacles) and the liveness specification ϕ_{liveness} for reaching the goal (green area).

heading direction. The discrete-time dynamics of the robot is given by:

$$\begin{aligned}\zeta_x^{(t+\Delta t)} &= \zeta_x^{(t)} + \Delta t v \cos(\theta^{(t)}) \\ \zeta_y^{(t+\Delta t)} &= \zeta_y^{(t)} + \Delta t v \sin(\theta^{(t)}) \\ \theta^{(t+\Delta t)} &= \theta^{(t)} + \Delta t u^{(t)}\end{aligned}\quad (21)$$

where the control input $u^{(t)} \in \mathbb{R}$ is determined by a ReLU NN controller, i.e., $u^{(t)} = \text{NN}(x^{(t)})$, $\text{NN} \in \mathcal{P}^{K \times b} \subset \mathbb{R}^{1 \times 4}$ with the controller space $\mathcal{P}^{K \times b}$ considered to be a hyperrectangle. We choose discrete time step size $\Delta t = 0.1$.

We considered two different workspaces indexed by 1 and 2 as shown in the upper and lower row of Figure 3, respectively. As the first step of our algorithm, we discretized the state space $\mathcal{X} \subset \mathbb{R}^3$ and the controller space $\mathcal{P}^{K \times b} \subset \mathbb{R}^{1 \times 4}$ as described in Section IV-A. To illustrate the flexibility in the choice of partition strategies, we partitioned the state space corresponding to workspace 1 uniformly into 552 abstract states, while partitioning the state space corresponding to workspace 2 non-uniformly into 904 abstract states. In both cases, the range of heading direction $\theta \in [0, 2\pi)$ is uniformly partitioned into 8 intervals, and the partitions of the x , y dimensions are shown as the dashed lines in the workspaces in Figure 3. We uniformly partitioned $\mathcal{P}^{K \times b}$ into 160 hyperrectangles.

By computing the reachable sets using the reachability tool TIRA [35], we constructed the posterior graph S_{Post} , which is then used to find the set of safe abstract states \mathbb{X}_{safe} and the function P_{safe} . The number of safe abstract states $|\mathbb{X}_{\text{safe}}|$ is 400 and 632 for workspaces 1 and 2, respectively. Notice that not all abstract states are safe. Indeed, abstract states that

are next to the obstacles with the heading direction θ towards the obstacles are inevitably unsafe, since the control input u cannot affect the coordinates ζ_x , ζ_y in one time step. The execution time to compute the posterior graph and to identify the set of safe states can be found in Table I.

We collected training data by following Algorithm 2 in Section V-A. We used Keras [38] to train a shallow NN (one hidden layer) with 4 hidden layer neurons for each abstract state $q \in \mathbb{X}_{\text{safe}}$. At the end of training, we projected the trained NN weights only once as mentioned in Section IV-D. For workspace 1, it takes 367 seconds to collect all the training data, and 463 seconds to train all the local NNs including the projection of the NN weights. For workspace 2, the execution time for collecting data is 601 seconds, and the total time for training and projection is 695 seconds.

In Figure 3, we show some trajectories under NN controllers trained by our algorithm in both workspaces. Despite we choose trajectories with initial states in the set $\mathcal{X}_{\text{init}} = \bigcup_{q \in \mathbb{X}_{\text{safe}}} q$ to be close to the obstacles or initially heading towards the obstacles, all the trajectories are collision-free as guaranteed by our algorithm. Moreover, by assigning controller partitions based on strategies in Section V-A, all trajectories satisfy the liveness specification ϕ_{liveness} .

Next, we compare NN controllers trained by our algorithm with those trained by standard imitation learning, which minimizes the regression loss without taking into account the safety guarantee. All NN controllers are trained using the same set of the training data. We vary the NN architectures for the NNs trained by standard imitation learning to achieve better performance, and train them using enough episodes for the loss

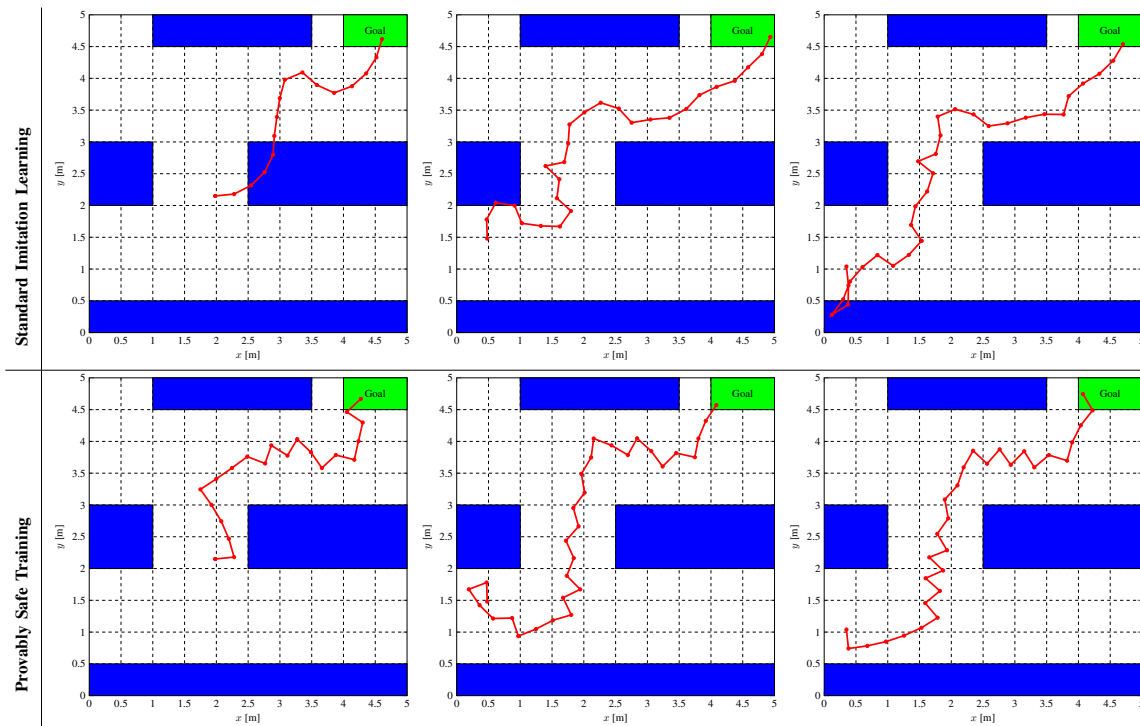


Fig. 4: The upper row shows trajectories resulting from NN controllers trained using standard imitation learning, where the NN architectures are (left) 2 hidden layers with 10 neurons per layer, (middle) 2 hidden layers with 64 neurons per layer, and (right) 3 hidden layers with 128 neurons per layer. The lower row shows trajectories resulting from NN controllers trained using our algorithm. With the same initial states (two sub-figures in the same column), only the NN controllers trained by our algorithm result into collision-free trajectories.

to be low enough. Nevertheless, as shown in Figure 4, for all the NN controllers trained by standard imitation learning, we are able find initial states starting from which the trajectories are not safe. However, with the same initial states, trajectories under NN controllers trained by our algorithm are collision-free, which is guaranteed by our framework.

B. Scalability Study

1- Scalability with respect to Partition Granularity: Our algorithm computes the reachable sets of abstract states under different controller partitions using reachability tools, which may employ conservative approximation for nonlinear systems. In that case, identifying the set of safe abstract states need finer partitioning of the state space \mathcal{X} and the controller space $\mathcal{P}^{K \times b}$. To that end, we show scalability of our algorithm with respect to the choice of partition parameters. Using the two workspaces in Figure 3, we increase the number of abstract states and controller partitions by decreasing the partition grid size and report the execution time for each part of our framework in Table I. As shown in the table, with finer partitioning of the state space (more abstract states), the number of safe abstract states increases. In this example, finer partitioning of the controller space does not lead to more safe abstract states, since controller partitions have been small enough and as mentioned above, some abstract states are inevitably unsafe. Moreover, we notice that the execution

TABLE I: Scalability with respect to Partition Granularity

| Workspace Index | Number of Abstract States | Number of Controller Partitions | Number of Safe & Reachable Abstract States | Compute Reachable Sets [s] | Construct Posterior Graph [s] | Compute Function P_{safe} [s] | Assign Controller Partitions [s] |
|-----------------|---------------------------|---------------------------------|--|----------------------------|-------------------------------|---------------------------------|----------------------------------|
| 1 | 552 | 160 | 400 | 52.6 | 82.3 | 0.06 | 0.7 |
| 1 | 552 | 320 | 400 | 107.5 | 160.3 | 0.1 | 0.9 |
| 1 | 552 | 640 | 400 | 223.1 | 329.6 | 0.2 | 1.7 |
| 1 | 1104 | 160 | 800 | 108.2 | 333.0 | 0.2 | 2.3 |
| 1 | 1104 | 320 | 800 | 219.6 | 684.2 | 0.4 | 2.7 |
| 1 | 1104 | 640 | 800 | 451.5 | 1297.4 | 0.6 | 4.2 |
| 2 | 904 | 160 | 632 | 88.1 | 159.1 | 0.1 | 1.0 |
| 2 | 904 | 320 | 632 | 203.6 | 313.2 | 0.2 | 1.1 |
| 2 | 904 | 640 | 632 | 393.2 | 660.8 | 0.3 | 1.7 |
| 2 | 1808 | 160 | 1264 | 202.1 | 634.6 | 0.3 | 3.4 |
| 2 | 1808 | 320 | 1264 | 388.6 | 1298.1 | 0.6 | 4.0 |
| 2 | 1808 | 640 | 1264 | 778.2 | 2564.4 | 0.9 | 5.9 |

time grows linearly with the number of abstract states and the number of controller partitions.

Although we conducted all the experiments on a single CPU core, we note that our algorithm can be highly parallelized. For example, computing reachable sets of the abstract states, checking intersection between the posteriors and the abstract states when constructing the posterior graph, and training local neural networks NN_q can all be done in parallel. After training the NN controller, the execution time of the controller is almost instantaneous, which is a major advantage of NN controllers.

2- Scalability with respect to System Dimension: Abstraction-based controller design is known to be computationally expensive for high-dimensional systems due to the curse of dimensionality. In Table II, we show scalability of our algorithm with respect to the system dimension. To conveniently increase the system dimension, we consider a chain of integrators represented as the linear system $x^{(t+1)} = Ax^{(t)} + Bu^{(t)}$,

TABLE II: Scalability with respect to System Dimension

| System Dimension n | Number of Abstract States | Compute Reachable Sets [s] | Construct Posterior Graph [s] |
|----------------------|---------------------------|----------------------------|-------------------------------|
| 2 | 69 | 0.6 | 0.7 |
| 4 | 276 | 2.7 | 2.6 |
| 6 | 1104 | 11.7 | 34.2 |
| 8 | 4416 | 57.1 | 521.0 |
| 10 | 17664 | 258.1 | 9840.4 |

where $A \in \mathbb{R}^{n \times n}$ is the identity matrix, and $u^{(t)} \in \mathbb{R}^2$. With fixed number of controller partitions and partition grid size for abstract states, Table II shows that the number of abstract states and execution time grow exponentially with the system dimension n . Nevertheless, our algorithm can handle a high-dimensional system in a reasonable amount of time.

REFERENCES

- [1] W. Saunders, G. Sastry, A. Stuhlmüller, and O. Evans, “Trial without error: Towards safe reinforcement learning via human intervention,” in *Proceedings of the 17th International Conference on Autonomous Agents and MultiAgent Systems*, 2018, pp. 2067–2069.
- [2] A. Liu, G. Shi, S.-J. Chung, A. Anandkumar, and Y. Yue, “Robust regression for safe exploration in control,” *arXiv preprint arXiv:1906.05819*, 2019.
- [3] F. Berkenkamp, A. Krause, and A. P. Schoellig, “Bayesian optimization with safety constraints: safe and automatic parameter tuning in robotics,” *arXiv preprint arXiv:1602.04450*, 2016.
- [4] P. Pauli, A. Koch, J. Berberich, and F. Allgöwer, “Training robust neural networks using lipschitz bounds,” *arXiv preprint arXiv:2005.02929*, 2020.
- [5] C. Gaskett, “Reinforcement learning under circumstances beyond its control,” 2003.
- [6] T. M. Moldovan and P. Abbeel, “Safe exploration in markov decision processes,” *arXiv preprint arXiv:1205.4810*, 2012.
- [7] M. Turchetta, F. Berkenkamp, and A. Krause, “Safe exploration in finite markov decision processes with gaussian processes,” in *Advances in Neural Information Processing Systems*, 2016, pp. 4312–4320.
- [8] L. Wen, J. Duan, S. E. Li, S. Xu, and H. Peng, “Safe reinforcement learning for autonomous vehicles through parallel constrained policy optimization,” *arXiv preprint arXiv:2003.01303*, 2020.
- [9] F. Berkenkamp, M. Turchetta, A. Schoellig, and A. Krause, “Safe model-based reinforcement learning with stability guarantees,” in *Advances in neural information processing systems*, 2017.
- [10] Y. Chow, O. Nachum, A. Faust, E. Duenez-Guzman, and M. Ghavamzadeh, “Lyapunov-based safe policy optimization for continuous control,” *arXiv preprint arXiv:1901.10031*, 2019.
- [11] Y. Chow, O. Nachum, E. Duenez-Guzman, and M. Ghavamzadeh, “A lyapunov-based approach to safe reinforcement learning,” in *Advances in neural information processing systems*, 2018, pp. 8092–8101.
- [12] T. Koller, F. Berkenkamp, M. Turchetta, and A. Krause, “Learning-based model predictive control for safe exploration,” in *2018 IEEE Conference on Decision and Control (CDC)*. IEEE, 2018.
- [13] X. Sun, H. Khedr, and Y. Shoukry, “Formal verification of neural network controlled autonomous systems,” in *Proceedings of the 22nd ACM International Conference on Hybrid Systems: Computation and Control*, 2019, pp. 147–156.
- [14] S. Dutta, S. Jha, S. Sankaranarayanan, and A. Tiwari, “Output range analysis for deep feedforward neural networks,” in *NASA Formal Methods Symposium*. Springer, 2018.
- [15] C. Liu, T. Arnon, C. Lazarus, C. Barrett, and M. J. Kochenderfer, “Algorithms for verifying deep neural networks,” *arXiv preprint arXiv:1903.06758*, 2019.
- [16] M. Fazlyab, A. Robey, H. Hassani, M. Morari, and G. Pappas, “Efficient and accurate estimation of lipschitz constants for deep neural networks,” in *Advances in Neural Information Processing Systems*, 2019, pp. 11 423–11 434.
- [17] W. Xiang, D. M. Lopez, P. Musau, and T. T. Johnson, “Reachable set estimation and verification for neural network models of nonlinear dynamic systems,” in *Safe, Autonomous and Intelligent Vehicles*. Springer, 2019, pp. 123–144.
- [18] R. Ivanov, J. Weimer, R. Alur, G. J. Pappas, and I. Lee, “Verisig: verifying safety properties of hybrid systems with neural network controllers,” in *Proceedings of the 22nd ACM International Conference on Hybrid Systems: Computation and Control*, 2019, pp. 169–178.
- [19] A. K. Akametalu, J. F. Fisac, J. H. Gillula, S. Kaynama, M. N. Zeilinger, and C. J. Tomlin, “Reachability-based safe learning with gaussian processes,” in *53rd IEEE Conference on Decision and Control*. IEEE, 2014, pp. 1424–1431.
- [20] V. Govindarajan, K. Driggs-Campbell, and R. Bajcsy, “Data-driven reachability analysis for human-in-the-loop systems,” in *2017 IEEE 56th Annual Conference on Decision and Control (CDC)*. IEEE, 2017, pp. 2617–2622.
- [21] J. F. Fisac, A. K. Akametalu, M. N. Zeilinger, S. Kaynama, J. Gillula, and C. J. Tomlin, “A general safety framework for learning-based control in uncertain robotic systems,” *IEEE Transactions on Automatic Control*, vol. 64, no. 7, pp. 2737–2752, 2018.
- [22] J. Ferlez, M. Elnaggar, Y. Shoukry, and C. Fleming, “Shieldnn: A provably safe nn filter for unsafe nn controllers,” *arXiv preprint arXiv:2006.09564*, 2020.
- [23] R. Cheng, G. Orosz, R. M. Murray, and J. W. Burdick, “End-to-end safe reinforcement learning through barrier functions for safety-critical continuous control tasks,” in *Proceedings of the AAAI Conference on Artificial Intelligence*, vol. 33, 2019, pp. 3387–3395.
- [24] K. P. Wabersich and M. N. Zeilinger, “Scalable synthesis of safety certificates from data with application to learning-based control,” in *2018 European Control Conference (ECC)*. IEEE, 2018, pp. 1691–1697.
- [25] M. Srinivasan, A. Dabholkar, S. Coogan, and P. Vela, “Synthesis of control barrier functions using a supervised machine learning approach,” *arXiv preprint arXiv:2003.04950*, 2020.
- [26] A. J. Taylor, A. Singletary, Y. Yue, and A. D. Ames, “A control barrier perspective on episodic learning via projection-to-state safety,” *arXiv preprint arXiv:2003.08028*, 2020.
- [27] X. Li and C. Belta, “Temporal logic guided safe reinforcement learning using control barrier functions,” *arXiv preprint arXiv:1903.09885*, 2019.
- [28] R. Cheng, M. J. Khojasteh, A. D. Ames, and J. W. Burdick, “Safe multi-agent interaction through robust control barrier functions with learned uncertainties,” *arXiv preprint arXiv:2004.05273*, 2020.
- [29] L. Wang, E. A. Theodorou, and M. Egerstedt, “Safe learning of quadrotor dynamics using barrier certificates,” in *2018 IEEE International Conference on Robotics and Automation (ICRA)*. IEEE, 2018, pp. 2460–2465.
- [30] A. Robey, H. Hu, L. Lindemann, H. Zhang, D. V. Dimarogonas, S. Tu, and N. Matni, “Learning control barrier functions from expert demonstrations,” *arXiv preprint arXiv:2004.03315*, 2020.
- [31] G. Shi, X. Shi, M. O’Connell, R. Yu, K. Azizzadenesheli, A. Anandkumar, Y. Yue, and S.-J. Chung, “Neural lander: Stable drone landing control using learned dynamics,” in *2019 International Conference on Robotics and Automation (ICRA)*. IEEE, 2019, pp. 9784–9790.
- [32] R. Pascanu, G. Montufar, and Y. Bengio, “On the number of response regions of deep feed forward networks with piece-wise linear activations,” *arXiv preprint arXiv:1312.6098*, 2013.
- [33] B. Yordanov, J. Tumova, I. Cerna, J. Barnat, and C. Belta, “Temporal logic control of discrete-time piecewise affine systems,” *IEEE Transactions on Automatic Control*, vol. 57, no. 6, pp. 1491–1504, 2012.
- [34] J. Ferlez, X. Sun, and Y. Shoukry, “Two-level lattice neural network architectures for control of nonlinear systems,” *arXiv preprint arXiv:2004.09628*, 2020.
- [35] P.-J. Meyer, A. Devonport, and M. Arcak, “Tira: toolbox for interval reachability analysis,” in *Proceedings of the 22nd ACM International Conference on Hybrid Systems: Computation and Control*, 2019, pp. 224–229.
- [36] A. Domahidi and J. Jerez, “Forces professional,” Embotech AG, url=https://embotech.com/FORCES-Pro, 2014–2019.
- [37] A. Zanelli, A. Domahidi, J. Jerez, and M. Morari, “Forces nlp: an efficient implementation of interior-point... methods for multistage nonlinear nonconvex programs,” *International Journal of Control*, pp. 1–17, 2017.
- [38] F. Chollet *et al.*, “Keras,” <https://keras.io>, 2015.